3D electrical resistivity tomography technique for the investigation of a construction and demolition waste landfill site

3D electrical resistivity tomography technique for the investigation of a construction and demolition waste landfill site

G. Vargemezis [1*] P. Tsourlos[1] A. Giannopoulos [2] P. Trilyrakis[3]

[1]Geophysical Laboratory, Department of Geophysics, Aristotle University of Thessaloniki, 54124 Thessaloniki, Greece

[2]Institute for Infrastructure and Environment, School of Engineering, The University of Edinburgh, EH9 3JL Edinburgh, UK

[3]TRILYRAKIS S.A., Alamanas 50 & K.Karamanli, 55132 Kalamaria, Thessaloniki, Greece

*Corresponding author: varge@geo.auth.gr

Abstract

This paper presents the practical application of a 3D electrical resistivity tomography (ERT) geophysical survey conducted in order to calculate the geometrical features and general structure of a construction and demolition waste layer in an old unregulated landfill prior to redevelopment. As traditional geological/geotechnical investigations comprised of cone penetration tests (CPT) failed to provide reliable results, primarily due to the nature of the underlying waste, a geophysical investigation was commissioned and found to be very effective in providing useful and accurate information to the project's environmental and engineering team. The ERT survey data were collected in parallel equidistant lines and were subsequently merged and inverted as a single 3D dataset. The processed data depicted clearly the interface between the resistive construction waste and the conductive undisturbed host clay layer ranging at depths between 3 and 11 meters. As a result of this successful geophysical investigation the total volume of the solid waste materials was calculated to be about 32,500m^3. Following the complete removal of the waste it became evident that the ERT geophysical survey results were particularly accurate. As a result, the reclamation constructor was able to carefully plan the required resources for excavating, moving and disposing of the waste. Interpreted ERT data not only defined the thickness of the debris layer and the total volume with a deviation of less than 10%, but also revealed the inner structure of the solid waste layer.

Keywords: Electrical resistivity tomography, construction and demolition waste landfill, geotechnical investigation.

Introduction

Redevelopment of old landfills is a challenging task since it is related to high environmental and geotechnical risks (Emberton and Parker, 1987). In the case of construction and demolition waste landfills the degree of environmental and health risk is reduced since most of the waste material can be considered as inert (Merino *et al*., 2010), yet still there is a possibility of the existence of hazardous materials (e.g. asbestos products, tar, paint etc.) which can also exhibit a degree of leachability (Townsend *et al*., 1999). This type of waste is commonly disposed to open liner landfills although, in some cases, a significant part is recycled (Merino *et al.*, 2010). Given the less hazardous nature of construction and demolition waste to health and the environment, in many countries, as well as in Greece, there is no well-organized collection and recycling facilities and therefore significant quantities of demolition waste are disposed in an uncontrolled manner (Fatta *et al*., 2003).

The reuse of particular construction and demolition waste sites requires the removal of the waste layer prior to any development actions for both environmental health and geotechnical reasons, since the direct construction of structures over such landfills have significant engineering difficulties as well as environment and potential human health risks. Since the prevailing environmental and geotechnical conditions, are very important parameters in relation to the constructability and safety of new build projects in old landfills careful site investigation is required prior to planning of redevelopment of such a waste site. Such an investigation includes any available historical information concerning previous land use in order to ensure both geotechnical (e.g. soil stability) and environmental safety (e.g. existence of hazardous waste).

Unfortunately, in many cases accurate information about the near surface geological formations is incomplete. Therefore, underground conditions that might affect the design must be clearly and conclusively investigated. This usually involves field and laboratory work concerning geological parameters, soil engineering properties and other relevant environmental and geotechnical parameters.

The present case study refers to the construction of a complex of houses in the area of "Thermi", near the city of Thessaloniki in Northern Greece (see Figure 1a). The top

sediments in the wider area are mostly red clays (Kockel *et al.* 1970). The particular plot of land, covering an area of about of 6000 m^2, had been used over many decades as a clay quarry in order to provide the raw material for the ceramics industry. However, all clay extraction pits had by the time of this investigation been refilled by solid waste materials. These materials were either by-products of the ceramic industry processing procedure, or they were demolition debris coming from nearby construction sites. Eventually, the initial clay quarry was fully refilled and leveled and at a later stage was acquired by a construction company for a housing development. As the entire quarrying-refilling procedure was at the time unregulated and no records were kept, the current owners of the site had to proceed to a detailed pre-investigation of the area by conducting a geotechnical survey.

This initial survey entailed a number of cone penetration tests (CPT). After fourteen CPTs had been performed, analysis of their results and in combination with their sparse distribution over the area indicated clearly that the problem was far more complex than it was originally anticipated. Therefore, it became evident that a more reliable investigative method, that could also provide more spatially dense information about the volume of the debris and the location of the undisturbed host rock, was needed. In this context the electrical resistive tomography (ERT) method was considered the most appropriate geophysical method.

Among others, geoelectrical methods are routinely used in investigating the inner structure of landfills (Chiampo *et al*., 1996; Porsani *et al*., 2004;) since the electrical properties of the waste materials and related leachates are clearly distinct form the ones of the underlying geological formations. Electrical resistivity tomography techniques are currently one of the most popular tools for near surface investigations (Loke *et al*., 2013) and has been widely used to map waste disposal sites (Tabbagh *et al.* 2000; Guerin *et al.* 2004; Soupios *et al*., 2007a; Matasovic *et al*., 2008; Seger *et al*. 2009).

The development of fully automated measuring devices and data processing/interpretation algorithms comprised a breakthrough innovation in geoelectrical exploration (Stummer, 2003). Automated data collection made possible the time-efficient acquisition of fully three-dimensional (3D) apparent resistivity data, by placing current electrodes on the nodes of a rectangular grid and measuring all the

possible potentials (Loke and Barker, 1996). Unfortunately, due to limitations often imposed by logistics, even today the most common practice to record the 3D subsurface apparent resistivity variation is through the application of dense parallel and/or orthogonal surface two-dimensional (2D) lines (Yi *et al*. 2001; Chambers, *et al*., 2002). This approach has been studied in detail by many authors (Papadopoulos *et al*.,2006; Gharibi and Bentley 2005). They have shown that 3D inversion of dense 2D ERT lines is certainly a surrogate to a full 3D survey and in many times the only fully 3D survey that someone can perform given instrumentation and logistic limitations.

For this reasons this approach for 3D geoelectrical surveying is widespread in geophysical practice (Negri *et al*., 2008; Drahor *et al*., 2008; Aizebeokhai et al., 2010). In particular this 3D approach has been used into mapping the structure of different waste disposal sites (Dahlin *et al*., 2002; Chambers *et al*., 2006; Soupios *et al*., 2007b; Chambers *et al*., 2012).

In the present case, the main target was to discriminate the construction waste layer from the undisturbed host clay formation. The main problems posed at the planning stage of the ERT survey were:

a) The heterogeneity of the demolition debris as blocks of walls of old houses, wooden doors, household materials, pieces of iron, were all included within demolition debris.

b) The fact that solid waste materials from the ceramic industry, as a residue from processing, were also deposited in the opened pits. That meant that the electrical contrast of these materials with the lower host clay layer was expected to be low. The only significant difference between these two types of clay materials was expected to be cohesion. Therefore, the geological clay layer was expected to be more conductive than the waste material.

The geoelectrical survey comprised a network of dense ERT parallel lines which were processed in a fully 3D mode. The geophysical results were interpreted in relation to existing CPT and complementary data and eventually solid waste thickness maps based on ERT interpreted data were produced. The subsequent excavation of the site allowed us to cross-check geophysical findings with ground truth.

The Cone Penetration Tests survey

The original lithological sequence of the study area had been significantly disturbed by two concurrent activities that changed the natural structure of the subsurface. Originally, the top clayey geological formations most likely comprised by clays, sandy clay-sand silty clays (according to the local geological map) were removed and replaced by heterogeneous solid waste composed of demolition debris and waste material from the ceramic industry that operated the quarry. Initial but unverified information suggested that the solid waste thickness was on average about 6m thick but also that it exhibited large variability (e.g. thickness more than 10m at locations) due to the way that the process of clay removal had taken place. In order to get some information about the geotechnical properties of the subsoil, a comprehensive CPT geotechnical study was conducted. Static CPTs are widely acknowledged as a standard field test to collect data about the bearing capacity and the frictional resistance of soils, as well as to delineate soil lithologic changes (Lunne *et al.* 1997). CPT tests were conducted using a 20Tons penetrometer providing a stable speed of 2cm/s that allows the recording of the force applied to the cone. It also recorded the total power for the given stress on the column (head and stocks) into the ground and the force applied for the combined stress at the mantle and cone. Amongst other measurements, the resistance at the tip of the cone (qc) as well as the sleeve friction (F_s) between the cone and the ground were estimated along the depth of the penetration. As a final step of the CPT analysis, the friction ratio $F_r = F_s/qc$ was calculated and used as a tool for the estimation of the composition of the geological strata. It should be noted that, due to ground stiffness, the penetration depth was limited to 9.6m at maximum, since it was impossible to go any deeper.

Fourteen static CPTs (P1-P14, Figure 1b) have been conducted reaching depths between 2.2 and 9.6 meters. According to the results of the CPT geotechnical analysis, two formations made up the subsurface to the depths reached by the CPTs.

Formation ‘TE’: solid waste backfilling: The backfilling material consists mostly of building rubble (bricks, stones etc). It also contains lutuceous sandy loose sediments originating from the pottery industry. The material was just delivered on site by trucks and placed without proper planning and without being subjected to any compression

during its deposition. As a result, a highly inhomogeneous, loose material with randomly located sacks of other various materials should be expected. Further, the material exhibits high porosity and permeability, with the possible existence of voids. Overall, this is a very bad quality material as far as its geotechnical properties (compressibility and resistance) are concerned and thus cannot host the foundations of the future houses.

Formation 'CS': Consolidated sandy-silty clay: This is the host rock formation in which clay material is dominant and was the raw material used by the ceramics industry. The formation is dense and appears to exhibit geotechnical properties, which allow the potential safe foundation of houses.

In Table 1 the estimated thicknesses of the solid waste layer as obtained from the CPTs are presented. It should be noted that two of the tests (P3, P13) failed to estimate the thickness of the rubble due to the incapability of the penetrometer to go any deeper at these locations. This is explained by the fact that at some points the demolition debris was so dense and strong that it impeded the advancement of the probe and this can be regarded as a disadvantage of the CPT application in cases like this. In Figure 1b, some typical examples of the CPT results are presented. The vertical axis in the diagrams shows the elevation (A.S.L.) and the horizontal axis the tip resistance qc (expressed in MPa). The CPT measurements at point P8 are considered to represent a typical successful CPT since it penetrated the entire TE formation and clearly delineates the ceiling of the clayey CS formation. The criterion for marking the interface is that the applied pressure exceeded the level of 10MPa reaching up to 25MPa. Actually, a value of qc=10MPa was considered to be the typical threshold for noting the transition into the CS formation. However, the results from other locations are of less typical CPT cases. This had raised doubts about the final interpretation of the CPT data. In the case of P1, the interface is estimated at the elevation of 101.75m by interpreting the peak at this depth, but the qc curve is also peaking at an elevation of 102.9m exhibiting, in both cases, a resistance that reached the value of 25MPa. This ambiguity in the interpretation is also apparent at CPT P14. Furthermore, in the case of the CPT at position P3, the test clearly failed completely to locate the interface.

In summary, although the CPT geotechnical survey provided some useful information

about the lithology in the area, it did not manage to provide a relatively reliable estimation of the interface between the solid waste and the host rock. This was due to the fact that the waste material itself was highly inhomogeneous and because in several cases the estimation of the solid waste layer thickness was not possible due to the fact that solid demolition debris were not possible to be penetrated. It should be also noted that by its nature the technique provides point information, and despite the density of the grid measurements, the interpolation of a highly variable interface may be quite inaccurate. The ambiguity in the interpretation of the CPT geotechnical data and the requirement of additional reliable information at low cost has driven the construction company to seek the advice of geophysicists and to request that an ERT geophysical survey be carried out.

The Electrical Resistivity Tomography Geophysical Survey

The main objective of the electrical resistivity tomography method was to delineate the solid waste formation from the mostly clayey host rock. It was expected that the waste formation would be relatively more resistive when compared with the mostly clayey host rock. For the 6000m^2 study area, given the initial rough estimate of the solid waste layer thickness, the ERT investigation depth was set to be around 15 meters. The geophysical survey parameters were selected in a way that the desired depth of investigation was achieved and at the same time the area of interest was covered with a relatively high resolution measurement pattern. Taking into account the overall size of the area, a basic grid of 78m by 69m was realized on the ground with cells (and electrode spacing) of 3m (Figure 2, Group A). This survey design resulted in conducting 27 parallel ERT lines each one having a length of 69m with interline spacing of 3m. This meant that 24 electrodes were used in every ERT line.

At the northern part of the study area, an existing angular extension led the survey team to include a smaller second grid comprised of 4 parallel lines (Group B). A third set (Group C) of three ERTs of the same specifications (length 69m, electrodes separation 3m) was acquired perpendicularly to the main group of ERT lines (Group A) in order to supplement the main grid in this particular area which had somewhat reduced resolution. Similarly, this also should have had to be carried out for the other

side (SW part) of the Group A measurement grid but as this actual grid exceeded the area of interest this was not considered necessary.

ERT measurements were collected using an IRIS Syscal Pro instrument. The Pole-Dipole array in both forward and reverse modes was used with an inter-electrode separation of 3 meters having a total length of 69 meters and with a maximum pole-dipole separation of $n = 8$ while measurements were also repeated with dipole spacings of 3, 6 and 9 meters. The remote electrode was located at the distance of 500m to the west of the study area.

The geoelectrical data were initially inverted using a standard 2D smoothness constrained inversion algorithm (Tsourlos, 1995), which is based on a finite element method forward solver. Further, all individual 2D ERT data were merged in a single dataset and were processed in full 3D mode using the DC3DPRO software (). 3D Inversion results were obtained after 6 iterations and the total root-mean-square error was 2.1%.

As all field resistivity measurements convey information regarding the 3D subsurface resistivity distribution, effectively a data set of dense parallel 2D ERT lines when assembled can be treated in a fully 3D mode both in view of modeling and inversion and as such is not less 3D than any other 3D data set. Therefore, in our models the measurements and the resistivity changes and sensitivities are fully 3D.

Subsurface resistivity images produced from the 3D inversion are presented for both X-Z sections as well as in full 3D images. In Figure 3a and 3b a typical inverted section is presented. Inverted image in Figure 3a resulted from 2D inversion algorithm (DC2dPRO, Kim 2009, Yi *et al.* 2001) while in Figure 3b the respective section that was extracted from the 3D inversion is presented for comparison purposes. Although both images exhibit a generally similar resistivity structure they exhibit clear differences especially at the resistivity distribution of the waste layer.

The high contrast between the top solid waste layer and the underlying clay formation can be clearly depicted. A “rainbow” color scale has been used to discriminate the two formations (TE – solid waste and CS – host rock) where blue colors (up to the limit of 19 Ohm-m) correspond to the CS formation while green to purple colors correspond to the TE formation. It is clear, that the waste layer is very inhomogeneous

and locally appears to be quite conductive. This is expected especially considering the varying nature of the deposited material, which included the refilling material, which originally had been excavated from the same area. The interface between these formations is marked in Figure 3b (dotted line). Further, a deeper, more sandy formation, typically encountered in this region, can be seen at a depth of approximately 18m. The subsequent interpreted section is shown in Figure 3c. To illustrate the effect of the solid waste layer an additional ERT line was obtained in an area where the solid waste layer was absent. Inversion results are shown in Figure 3d and it is obvious that that the resistive top layer is now missing as resistivities are pretty low and do not exceed the 20 Ohm-m suggesting that this is a reasonable resistivity threshold for discriminating the waste layer

In Figure 4 selected ERT sections are presented together with the respective CPT logs in order to allow for comparisons. In all resistivity sections the interface between the CS and TE formations is clearly seen (isoresistivity line of 19 Ohmm). Comparisons between the ERT inversions and the CPT interpretations show only partial correlation. In particular, there is some good agreement between ERT Line 9 and CPTs P4 and P8 (Figure 4b). In some other cases CPTs seem to underestimate the thickness of the solid waste compared with the ERT interpretations (ERT14–P12, ERT2–P9 and P5). The CPTs P3 and P13 failed to reveal the interface. A special note should be made about CPT P14 (Figure 4c) which exhibits several layer changes as this coincides well with the high geoelectrical complexity of the solid waste material at this particular point as can be seen in the inverted image of ERT Line 2. Overall, it seems that the 3D inverted results have managed to depict the interface in a very convincing way. Data inversion allowed the construction of full 3D images where the volume of the resistive solid waste layer is represented (Figure 5).

The threshold between the two formations was decided to be the 19 Ohm-m isoresistive line on the basis of the inversion results of the line outside the waste area (Fig. 3d). The isoresistive line was subsequently digitized in the 3D inverted results in order to obtain the 3D variation of the thickness of the solid waste formation. Based on this process, the average thickness of the debris (TE formation) was estimated to be 6m with a range between 1.1 and 9 meters. In Figure 6a a map of the ERT estimated rubble layer thickness is presented. The purpose of producing these maps

was two-fold:

- To guide the construction company in their project planning for removing the debris and;

- To inform the change of the original plan of the buildings complex in order to adapt their locations and foundation elevations. The volume of the TE formation was calculated to be 32,500m^3. Obviously, this information proved to be very important to the construction company since it allowed them to obtain an estimate of the total costs involved in removing the rubble layer.

The excavation that took place a few months after the completion of the ERT survey revealed the actual structure of the subsurface and to a great degree verified the predictions of the geophysical survey. In Table 2 the ERT predictions of the rubble thickness are benchmarked against the actual excavation findings and CPT predictions for the specific locations. Further, in Figure 6 the ERT thickness map is compared against the actual and the CPT calculated ones (Figures 6a, 6b, 6c). It is clear that there is very good agreement between ground-truth and the geophysical predictions (average difference less than 1m) but this is not clearly the case for the CPT based map (average difference 2.4m where estimation was possible).

Discussion and Conclusions

It was important from the planning stage of the ERT survey that survey lines took into account the possibility of 3D inversion of the data which proved to be very useful in a highly variable and inhomogeneous site. Although, CPT geotechnical data were available, they were partly unreliable, so it was decided that the geoelectrical resistivity survey interpretation to be carried out independently. The high electrical resistivity contrast between the top solid waste layer and the clay host rock guided the interpretation and the setting of the resistivity threshold used to denote the interface between these two formations.

Comparisons between the CPT results and the geoelectrical sections were made only at the final stage of the evaluation. More importantly, the subsequent excavation of the landfill and the removal of the entire solid waste layer allowed direct comparisons with ground truth. The average difference between the ERT estimated and actual

thickness of the solid waste layer is 0.95 meter at a range between 0 and 2.5 meters. Further, the ERT predicted and actual values of the elevation of the predicted parental surface were correlated by the use of linear regression (Figure 7a). The regression coefficient in this case is 0.84 suggesting a very good correlation as opposed to the less satisfactory correlation achieved in the case of the CPT predicted values which was 0.44 (see Figure 7b).

Overall, given the final records of the construction company, as far as the total solid waste removal volume is concerned, the ERT predicted value deviated only 5% from the actual one (32.500m^3). Taking into account the heterogeneity of the topsoil of the area, the results of the resistivity survey concerning the resolution given by the measuring parameters are also quite satisfactory. As further evidence, a photograph of the excavation section at the SE side of the study area is presented in Figure 8a in which the interfaces between discrete layers of different materials are noted as white traced lines. This section coincides with part of the ERT1 section (see Figure 2 for location) and the respective resistivity image is also depicted in Figure 8b. The sack marked as A in the middle of the photo (Figure 8a) is a typical example of the way that trucks were depositing their debris in the chamber. The traces of the geological section are also transferred into the respective geoelectrical section (Figure 8b) and they correspond very well with the geoelectrical interfaces. Clay layers at the right show very low resistivity values while the gravel-based mixture on the left has very high resistivity values. The body in the middle which is demolition debris has an average resistivity between the two previous extreme examples. The general inclination of the geoelectrical interfaces represents realistically the actual layering of the solid waste structure.

In conclusion, the geoelectrical technique proved particularly successful since in this case did not only supplemented the preliminary survey but also has given very reliable results regarding the inner structure of the landfill which have informed and influenced the design of the actual project. It is noted that before excavation the constructors introduced modifications to their plan, based only on the geophysical results. This very successful practical application of ERT imaging demonstrates and reinforces the use of geophysical methods in complex site investigation and environmental problems.

References

Aizebeokhai, A. P., Olayinka, A. I. and Singh, V. S., 2010. Application of 2D and 3D geoelectrical resistivity imaging for engineering site investigation in a crystalline basement complex terrain southwestern Nigeria. Environmental Earth Sciences, 61, 1481 - 1492.

Chambers, J.E, Ogilvy, R.D., Kuras, O. and Meldrum, P.I. 2002. 3D Electrical Imaging of Known Targets at a Controlled Environmental Test Site. Environmental Geology, 41, 690-704.

Chambers, J., Kuras, O., Meldrum, P., Ogilvy, R., and Hollands, J., 2006. Electrical resistivity tomography applied to geologic, hydrogeologic, and engineering investigations at a former waste-disposal site. Geophysics, 71(6), B231–B239.

Chambers, J E, Wilkinson, P B, Wardrop, D, Hameed, A, Hill, I, Jeffrey, C, Loke, M H, Meldrum, P I, Kuras, O, Cave, M, Gunn, D A. 2012. Bedrock detection beneath river terrace deposits using three-dimensional electrical resistivity tomography. Geomorphology, Vol. 177-178, 17-25.

Chiampo F., Conti R., and Cometto D., 1996. Morphological characterization of MSW landfills. Resources, Conservation and Recycling 17, 37-45.

Dahlin T., Bernstone C. and Loke M-H., 2002. Case History : A 3-D resistivity investigation of a contaminated site at Lernacken, Sweden. Geophysics, 67, 1692-1700.

Drahor, M. G., Berge, M. A., Kurtulmuş, T. Ö., Hartmann, M. and Speidel, M. A., 2008. Magnetic and electrical resistivity tomography investigations in a Roman legionary camp site (Legio IV Scythica) in Zeugma, Southeastern Anatolia, Turkey. Archaeological Prospection, 15, 3, 159-186,

Emberton, J.R., and Parker A., 1987. The problems associated with building on landfill sites. Waste Management & Research, 5, 473-482.

Fatta D., Papadopoulos A., Avramikos E., Sgourou E., Moustakas K., Kourmoussis F., Mentzis A.,and Loizidou M.,2003. Generation and management of construction and demolition waste in Greece—an existing challenge. Resources, Conservation and Recycling,40, 81-91.

Guerin R., Begassat Ph., Benderitter Y., David J., Tabbagh A. and Thiry M. 2004. Geophysical study of the industrial waste land in Mortagne-du-Nord (France) using electrical resistivity. Near Surface Geophysics 3, 137–143

Gharibi, M. and Bentley, L.R. 2005. Resolution of 3-D Electrical Resistivity Images from Inversions of 2-D Orthogonal Lines. JEEG, 10, 4, 339-349.

Kim J. H. 2009. DC2DPro-2D interpretation system of DC resistivity tomography. UserYs Manual and Theory KIGAM, S. Korea

Kockel F., Mollat H., Antoniades P. H. and Papadopoulos P. 1970. Geological map of Greece Thermi Sheet, Scale. 1:50.000 IGME, Athens

Loke M. H. and Barker R. D. 1996. Practical techniques for 3D resistivity surveys and data inversion. Geophysical Prospecting 44. 499–523

Loke, M.H.,Chambers, J.E.,Rucker, D.F.,Kuras, O., Wilkinson, P.B., 2013. Recent developments in the direct-current geoelectrical imaging method. Journal of Applied Geophysics, 95, 135-156.

Lunne T., Robertson P. K. and Powell J. J. M. 1997. Cone Penetration Testing in Geotechnical Practice, Blackie Academic & Professional.

Merino, M., Gracia, P. and Azevedo, I., 2010. Sustainable construction: construction and demolition waste reconsidered. Waste Management & Research, 28, 118-129.

Matasovic N., El-Sherbiny R. and Kavazanjian, E., 2008. In-situ measurements of MSW properties. In Geotechnical Characterization, Field Measurement and Laboratory Testing of Municipal Solid Waste, D. Zekkos (edd), ASCE Geotechnical Special Publication No.209.

Negri, S., Leucci, G., and Mazzone, F. 2008. High resolution 3D ERT to help GPR data interpretation for researching archaeological items in a geologically complex subsurface. Journal of Applied Geophysics 65, 111-120.

Porsani J.L., Filhob, W.M., Vagner, R.E., Shimelesa, F., Douradob, J.C., and Moura, H.P., 2004. The use of GPR and VES in delineating a contamination plume in a landfill site: a case study in SE Brazil. J Appl Geophys 55,199–209.

Papadopoulos N. G., Tsourlos P., Tsokas G. N., Sarris A., 2006. Two-dimensional and three-dimensional resistivity imaging in archaeological site investigation.

Archaeological Prospection, 13, 163-181.

Seger M., Cousin I., Frison A. and Boizard H. and Richard G. 2009. Characterization of the structural heterogeneity of the soil tilled layer by using in situ 2D and 3D electrical resistivity measurements. Soil & Tillage research 103, 387–398

Soupios P, Papadopoulos I, Kouli M, Georgaki I, Vallianatos F, Kokkinou E, 2007a, Investigation of Waste Disposal Areas Using Electric Methods : A Case Study from Hania – Crete, Greece, Environmental Geology, 53,661-675.

Soupios P.M., Georgakopoulos P., Papadopoulos N., Saltas V., Andreadakis A, Vallianatos F., Sarris A.and J.P. Makris, 2007b. Use of engineering geophysics to investigate a site for a building foundation. Journal of Geophysics and Engineering 4 (1), 94-103, 2007.

Stummer, P. 2003. New Develpments in Electrical Resistivity Imaging. Dissertation submitted to the Swiss Federal of Institute of Technology, Zurich.

Tabbagh A., Dabas M., Hesse A. and Panissod C. 2000. Soil resistivity: a non-invasive tool to map soil structure horizonation. Geoderma 97, 393–404

Townsend, T., Jang, Y., and Thurn, L., 1999. Simulation of Construction and Demolition Waste Leachate. Journal of Environmentak Engineering, 125, 1071–1081.

Tsourlos P. 1995. Modelling, interpretation and inversion of multielectrode resistivity survey data. DPhil thesis. University of York

Yi M. J., Kim J. H., Song Y., Cho S. J. and Chung S. H. and Suh J. H. 2001. Three-Dimensional Imaging of Subsurface Structures using Resistivity Data. Geophysical Prospecting 49, 483 –497

List of Tables

Table 1. Depth and elevation of the ceiling of the original surface.

Table 2. Actual thickness of demolition debris, estimated by CPT and predicted by the ERT survey.

List of Figures

Figure 1. (a) Location of the study area, (b) Geotechnical survey. The locations of CPT measurements are shown as well as some characteristic examples of the data. In the graphs, the horizontal axis refers to the tip resistance (in MPa) while the vertical axis shows the elevation (in meters).

Figure 2. Layout of the survey area and the ERT lines.

Figure 3. Geological interpretation (c) of the geoelectrical model: (a) 2D inversion, (b) Section extracted from the 3D inversion of the geoelectrical data,(d) inversion results of a section just outside the waste area.

Figure 4. ERT 2D inversion together with the respective CPT results for sections (a) 14, (b) 9 and (c) 2.

Figure 5. ERT 3D inversion results in image format of the overall survey area. On the left, view from the South and on the right view from the West.

Figure 6. Solid waste thickness (a) ERT estimated, (b) actual and (c) CPT estimated.

Figure 7. Linear regression results for the correlation of verified solid waste thickness with the one estimated by CPT and ERT.

Figure 8. Excavated section at the eastern edge of the area along with the respective geoelectrical 2D section. Interfaces and debris sacks have been traced to showcase the debris sacks and the interfaces between layers of different materials.

CPT	*Penetration Depth (m)*	*Elevation (m)*	*CPT Estimated Thickness (TE)*	*CPT Estimated Elevation of Host rock (m)*
P1	3.2	104.75	3	101.75
P2	2.4	104.00	1.6	102.40
P3	6.0	106.30	?	-
P4	7.8	106.40	7.4	99.00
P5	2.2	106.45	2	104.45
P6	3.4	103.70	2.8	100.90
P7	8.8	106.33	8	98.33
P8	8.8	106.10	7.6	98.50
P9	3.8	106.10	3	103.10
P10	6.6	99.30	6	93.30
P11	3.4	100.50	3.2	97.30
P12	3.8	101.40	3	98.40
P13	4.0	103.20	?	-
P14	9.6	103.50	9	94.50

Table 1. Depth and elevation of the ceiling of the original surface.

CPT code	Thickness of demolition debris (m)			Difference	
	Actual	CPT	ERT	Act-CPT	Act-ERT
P1	3.8	3	3.5	0.8	0.3
P2	8.3	8	7.9	0.3	0.4
P3	8.5	7.6	6	0.9	2.5
P4	8.5	3	6.7	5.5	1.8
P5	3.3	6	2	-2.7	1.3
P6	5.7	3.2	5.9	2.5	-0.2
P7	6.4	3	8.5	3.4	-2.1
P8	7.9	-	7.9	7.9	0
P9	8.3	9	9	-0.7	-0.7
P10	4.4	1.6	4.8	2.8	-0.4
P11	7.1	-	7	7.1	0.1
P12	8	7.4	7.3	0.6	0.7
P13	8.5	2	7.3	6.5	1.2
P14	4.7	2.8	3.1	1.9	1.6

Table 2. Actual thickness of demolition debris, estimated by CPT and predicted by the ERT survey.

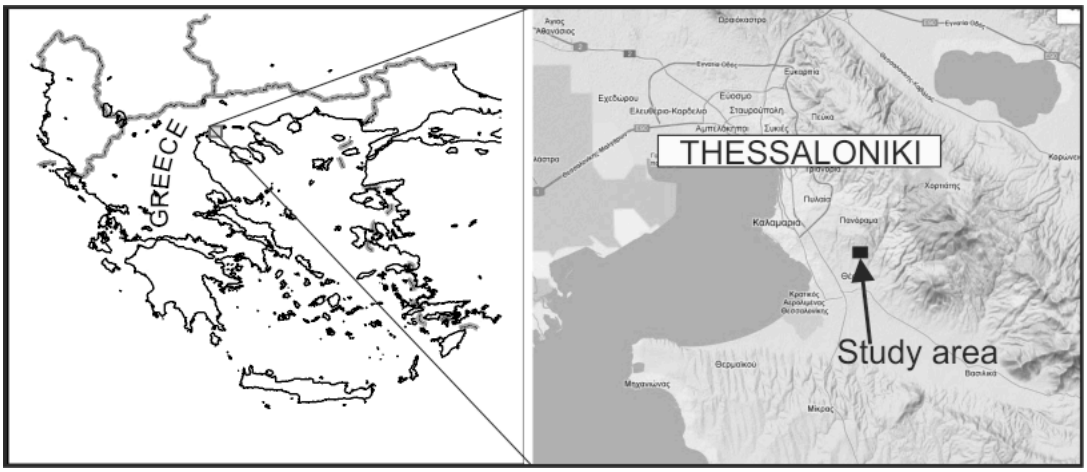

(a)

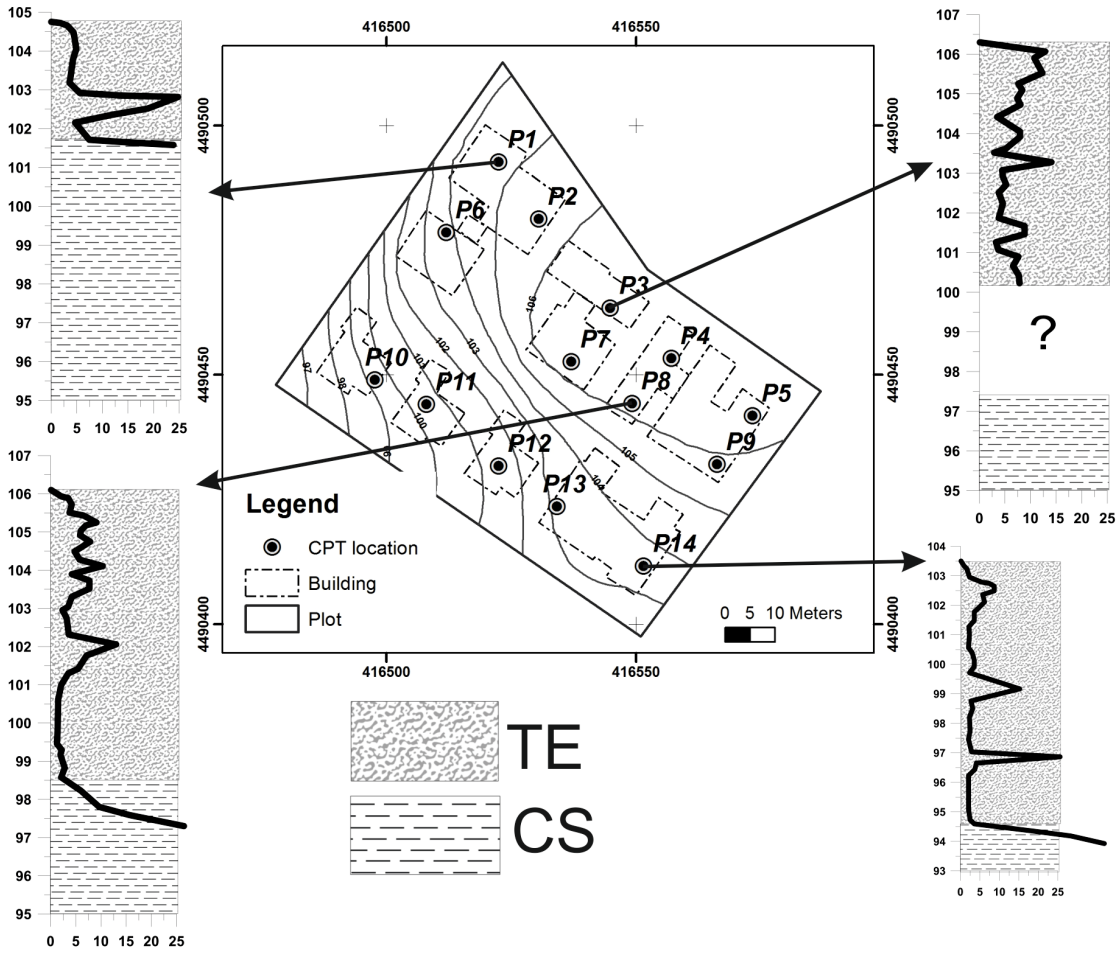

(b)

Figure 1. (a) Location of the study area, (b) Geotechnical survey. The locations of CPT measurements are shown as well as some characteristic examples of the data. In the graphs, the horizontal axis refers to the tip resistance (in MPa) while the vertical axis shows the elevation (in meters).

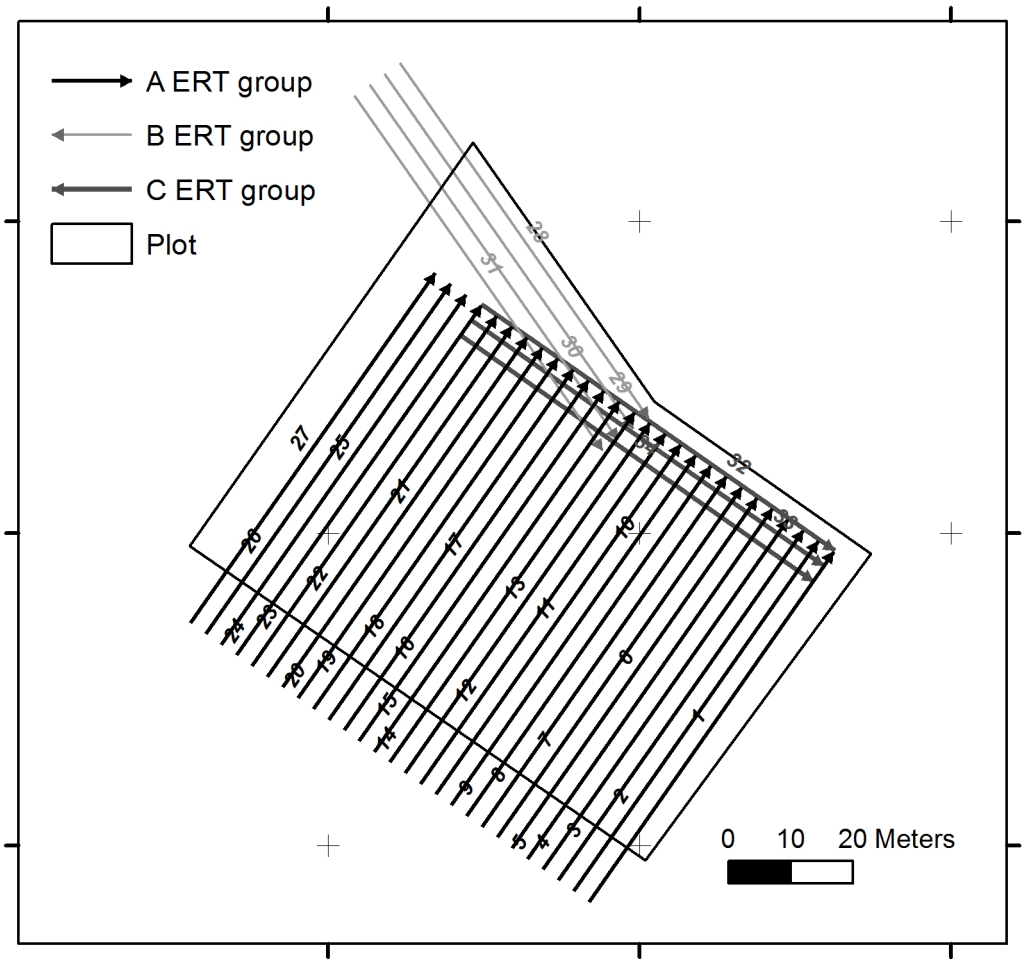

Figure 2. Layout of the survey area and the ERT lines.

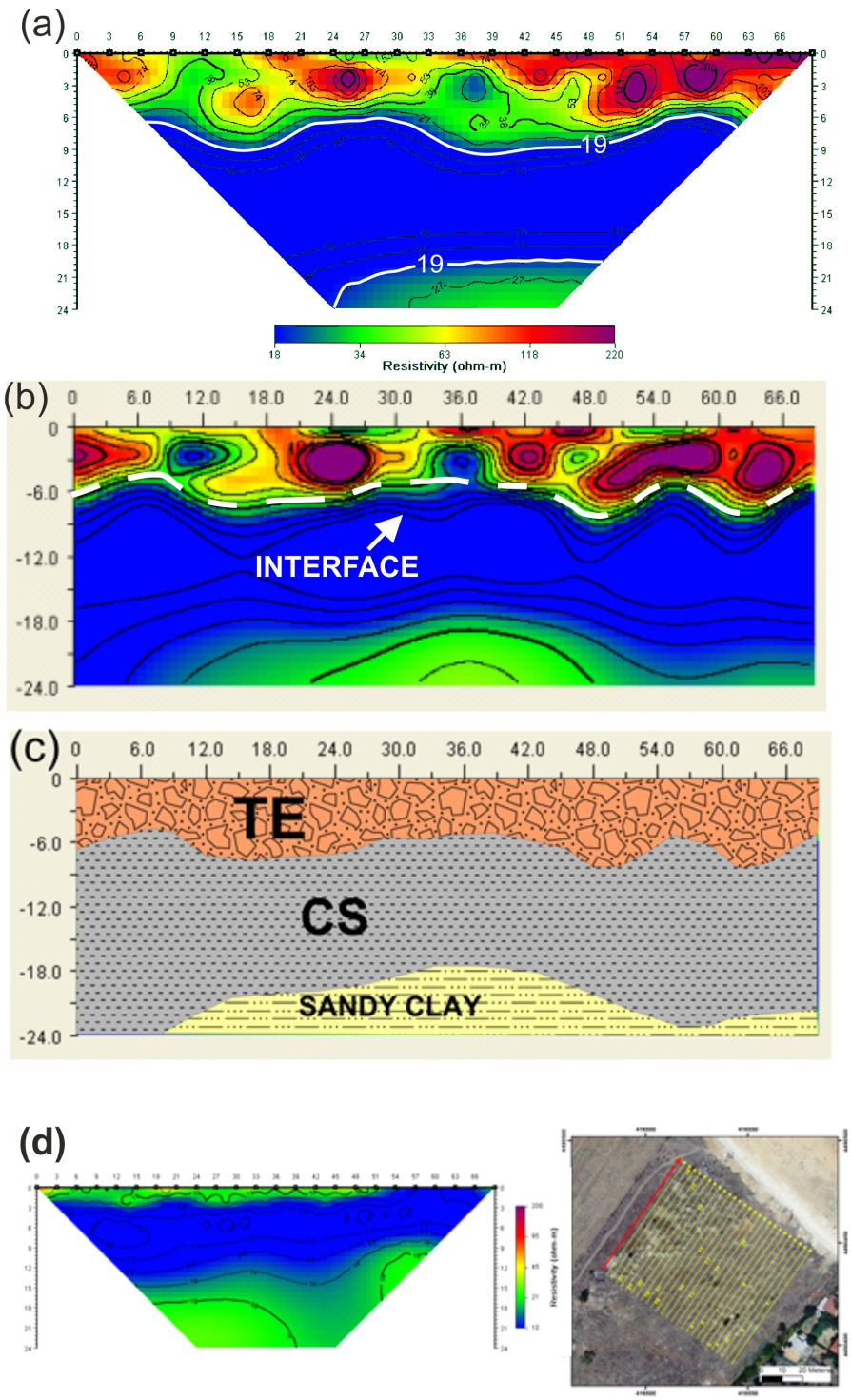

Figure 3. Geological interpretation (c) of the geoelectrical model: (a) 2D inversion, (b) Section extracted from the 3D inversion of the geoelectrical data, (d) inversion results of a section just outside the waste area.

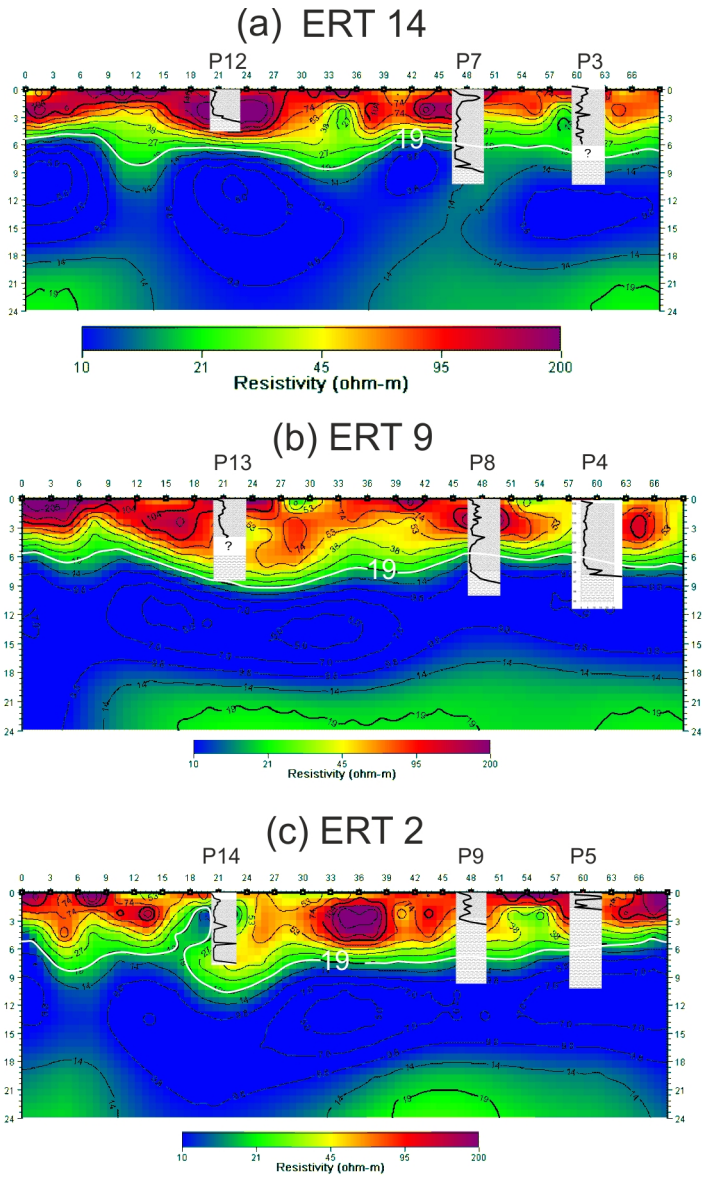

Figure 4. ERT 2D inversion together with the respective CPT results for sections (a) 14, (b) 9 and (c) 2.

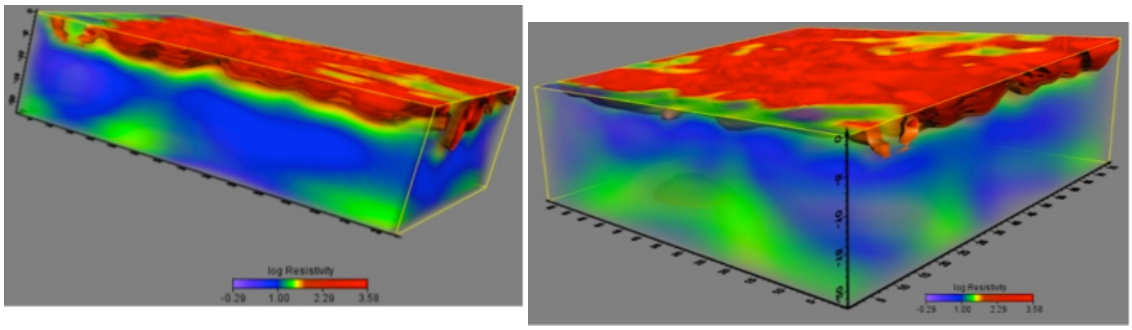

Figure 5. ERT 3D inversion results in image format of the overall survey area. On the left, view from the South and on the right view from the West.

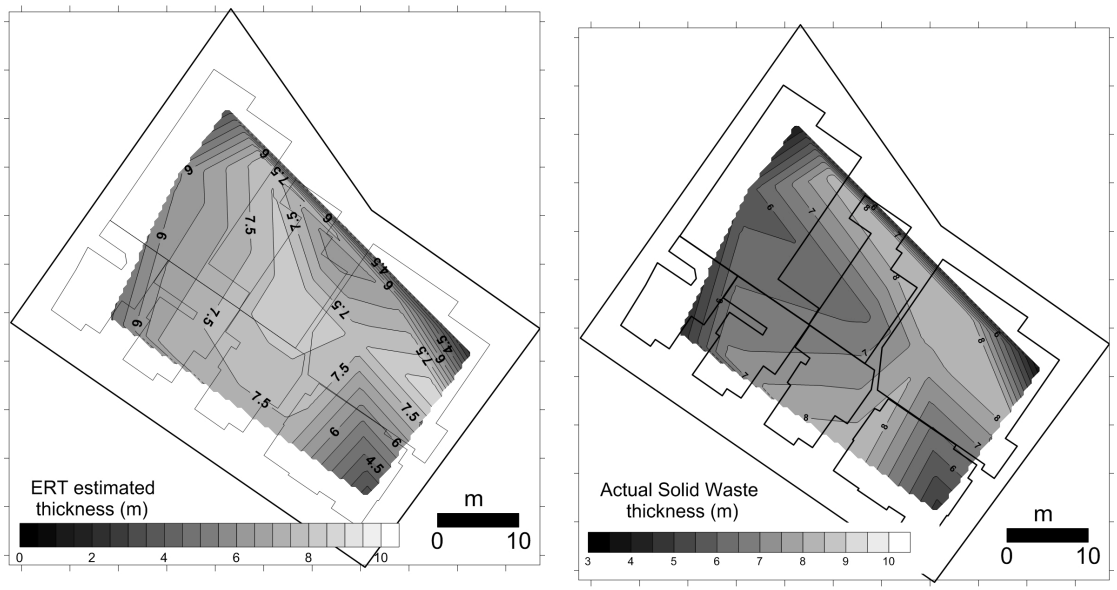

(a)

(b)

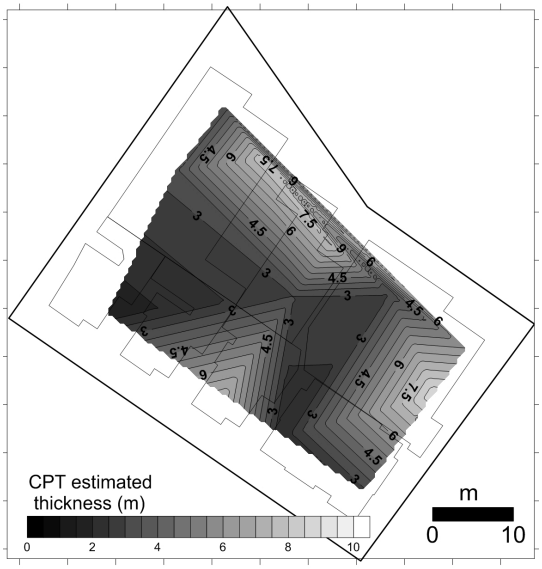

(c)

Figure 6. Solid waste thickness (a) ERT estimated, (b) actual and (c) CPT estimated.

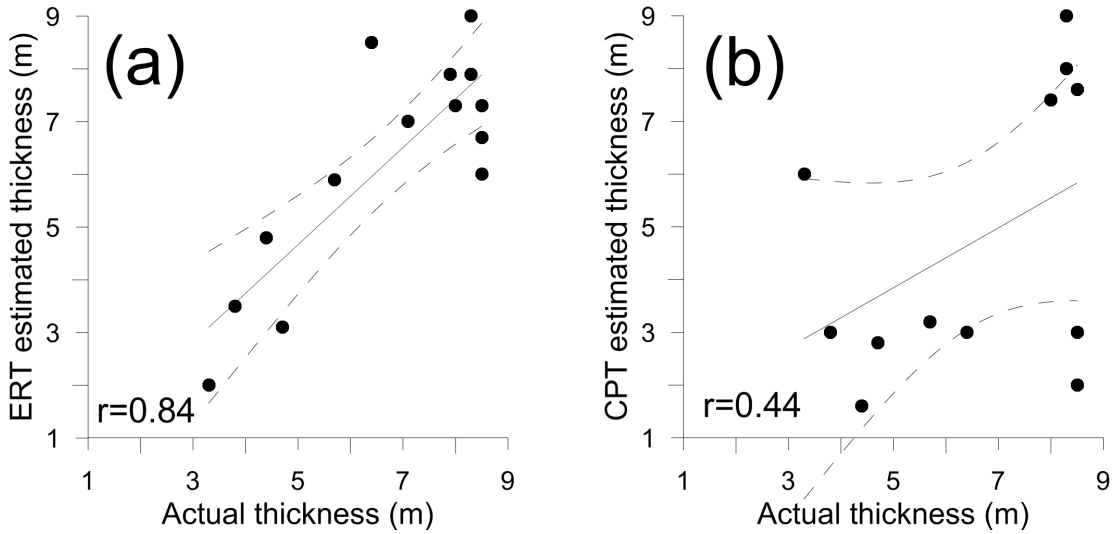

Figure 7. Linear regression results for the correlation of verified solid waste thickness with the one estimated by CPT and ERT.

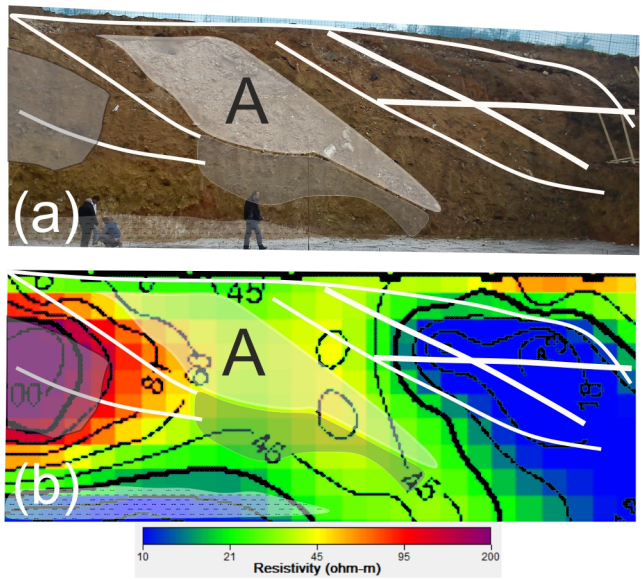

Figure 8. Excavated section at the eastern edge of the area along with the respective geoelectrical 2D section. Interfaces and debris sacks have been traced to showcase the debris sacks and the interfaces between layers of different materials.